

The Vev Flip-Flop: Dark Matter Decay between Weak Scale Phase Transitions

Michael J. Baker^{1,*} and Joachim Kopp^{1,†}

¹*PRISMA Cluster of Excellence & Mainz Institute for Theoretical Physics,
Johannes Gutenberg University, Staudingerweg 7, 55099 Mainz, Germany*

(Dated: July 18, 2022)

We propose a new alternative to the Weakly Interacting Massive Particle (WIMP) paradigm for dark matter. Rather than being determined by thermal freeze-out, the dark matter abundance in this scenario is set by dark matter decay, which is allowed for a limited amount of time just before the electroweak phase transition. More specifically, we consider dark matter particles coupled weakly to a scalar mediator S and a SM fermion. Dark matter freezes out while still relativistic, so its abundance is initially very large. As the Universe cools down, the scalar mediator develops a vacuum expectation value (vev), which breaks the \mathbb{Z}_2 symmetry that stabilises dark matter. This allows dark matter to mix with SM particles and decay. During this epoch, the dark matter abundance is reduced to give the value observed today. Later, the SM Higgs field also develops a vev, which feeds back into the S potential and restores the \mathbb{Z}_2 symmetry. In a concrete model we show that this “vev flip-flop” scenario is phenomenologically successful in the most natural regions of its parameter space. We also comment on detection prospects at the LHC and elsewhere, and on the implications for baryogenesis.

The WIMP (Weakly Interacting Massive Particle) paradigm in dark matter physics states that dark matter (DM) particles should have non-negligible couplings to Standard Model (SM) particles. Their abundance today would then be determined by their abundance at freeze-out, the time when the temperature of the Universe dropped to the level where interactions producing and annihilating DM particles become inefficient. In many models these interactions should still be observable today, through residual DM annihilation in galaxies and galaxy clusters, through scattering of DM particles on atomic nuclei, or through DM production at colliders. The conspicuous absence of any convincing signals [1–7] to date motivates us to look for alternatives to the WIMP paradigm.

In this letter, we present a scenario in which the DM abundance is set not by annihilation, but by decay. We focus on models in which fermionic DM particles couple to a new scalar species and argue that the resulting scalar potential may undergo multiple phase transitions, “flip-flopping” between phases in which the \mathbb{Z}_2 symmetry stabilising the DM is intact and a phase where it is broken. Similar behaviour is found in models of electroweak baryogenesis [8–12]. During the broken phase, the initially overabundant DM particles are depleted until their relic density reaches the value observed today. Although the resulting picture of early freeze out, followed by a period of DM decay around the weak scale, is quite generic, we focus here on a concrete example and comment on possible generalisations along the way.

Model Framework.—We introduce a complex dark sector scalar S with hypercharge -1 , similar to the right-handed stau in supersymmetry. We take the DM particle to be a Dirac fermion χ , uncharged under the SM gauge

group. Both S and χ are assumed to be odd under a \mathbb{Z}_2 symmetry that stabilises the DM and could be a remnant of a dark sector gauge symmetry broken at a scale $\gg \text{TeV}$. The tree level potential and the relevant terms in the Lagrangian of the model are

$$V^{\text{tree}} = -\mu_H^2 H^\dagger H + \lambda_H (H^\dagger H)^2 - \mu_S^2 S^\dagger S + \lambda_S (S^\dagger S)^2 + \lambda_p (H^\dagger H)(S^\dagger S), \quad (1)$$

$$\mathcal{L} \supset y_\tau \bar{L}_\tau H \tau_R^- + y_\chi S^\dagger \bar{\chi} \tau_R^- + h.c. - V^{\text{tree}}. \quad (2)$$

The first line contains the SM Higgs potential, characterised by the tree-level mass parameter $\mu_H \simeq 88 \text{ GeV}$ and the quartic coupling $\lambda_H \simeq 0.12$. We will use $H = (G^\pm, (h + iG^0)/\sqrt{2})$. The second line contains the analogous potential for the scalar mediator S , characterised by $\mu_S \sim \mathcal{O}(100 \text{ GeV})$ and a positive $\lambda_S \sim \mathcal{O}(1)$, along with a Higgs portal term with coupling $\lambda_p \sim \mathcal{O}(1)$. In the Lagrangian we highlight the SM Yukawa coupling between the Higgs field, the left-handed third-generation leptons L_τ , and the right-handed taus τ_R^- . The relation between the coupling constant y_τ and the τ mass is as usual $m_\tau = y_\tau v/\sqrt{2}$, where $v = 246 \text{ GeV}$ is the Higgs vacuum expectation value (vev) in the SM at zero temperature. We also introduce a new Yukawa coupling involving S , χ , and τ_R^- with coupling constant y_χ . We could straightforwardly generalise the model to include also the first and second generation of leptons, or we could make S neutral under hypercharge and consider couplings to right-handed neutrinos instead of τ leptons. We defer these generalisations to future work.

We assume that the parameters μ_H^2 , μ_S^2 , λ_H , λ_S and λ_p of the scalar potential are chosen such that, at zero temperature, the SM Higgs field has its usual vev $\langle H \rangle = (0, v/\sqrt{2})$, while $\langle S \rangle = 0$. Thus, the electroweak

symmetry is broken at temperature $T = 0$, while the \mathbb{Z}_2 symmetry that stabilises DM is unbroken. The tree level masses of the physical Higgs boson h and of S today are then given by $m_H^2 = 2\mu_H^2$ and $m_S^2 = -\mu_S^2 + \lambda_p \mu_H^2 / (2\lambda_H)$. We assume that $m_\chi < m_S$ at $T = 0$ to avoid DM decay via $\chi \rightarrow S + \tau$. If this decay channel was open, S would be the thermal relic and the situation would return to the usual scalar Higgs portal model [13–20].

The Vev Flip-Flop.—To determine the evolution of the system given by eq. (2) in the hot early Universe, we consider the effective potential V^{eff} . In addition to V^{tree} , the effective potential includes the T -independent one-loop Coleman–Weinberg contributions [21], the one-loop T -dependent corrections [22], and the resummed higher-order “daisy” contributions [23–26], see appendix A for details. We include the dominant contributions to these higher order terms from t, Z^μ, W^μ, H and S . We neglect the contribution from the coupling of S to the hypercharge gauge boson B^μ , which we found to be numerically small. The Coleman–Weinberg contribution introduces a renormalisation scale, which we set equal to the SM Higgs vev.

The features of V^{eff} depend on the parameter values chosen, but several generic points should be emphasised. Firstly, we should bear in mind that the masses of H and S , which are given by the second derivatives of the potential, will vary with temperature. This will become important when we consider χ decay. Secondly, at high temperature, the μ_S^2 receives negative contributions from the one-loop T dependent term, and positive contributions from the “daisy” terms. This means that at high T , the \mathbb{Z}_2 symmetry may be broken or unbroken, depending on which contribution dominates. Electroweak symmetry is always intact at high T for the experimentally determined values of μ_H^2 and λ_H .

We illustrate the main features of the flip-flopping vevs mechanism in fig. 1, for a specific choice of Lagrangian parameters as given in the figure caption. At high T (top left panel of fig. 1), the effective potential is symmetric in both S and H . As the Universe cools the T -dependent corrections to the S mass term become subdominant and, since μ_S^2 is positive, S develops a non-zero vev at $T = T_S$, fig. 1 (top right). Now the \mathbb{Z}_2 symmetry that stabilises χ is broken. The Yukawa coupling $y_\chi S^\dagger \bar{\chi} \tau_R^-$ leads to a mixing between χ and τ_R , and χ can decay, e.g., via $\chi \rightarrow L_\tau H$ or $\chi \rightarrow \tau_R B^\mu$. Note that, during this epoch, SM hypercharge is also broken and B^μ obtains a mass $m_B = \sqrt{2}g'\langle S \rangle$, where g' is the SM hypercharge coupling.

As the temperature continues to drop T -dependent corrections to μ_H become subdominant and V^{eff} develops new minima at non-zero $\langle H \rangle$. The extra contribution of this vev to the S^2 term through the Higgs portal makes the effective μ_S^2 negative and so $\langle S \rangle = 0$ is restored at the new minima. At first, the minima at $\langle H \rangle \neq 0$ are only local minima, but as the temperature drops they become

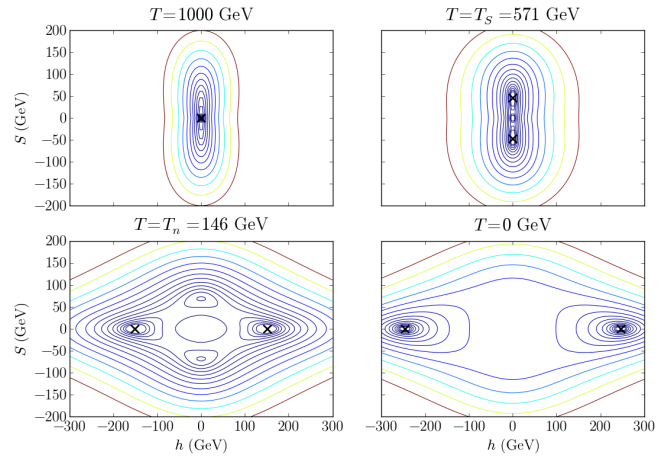


Figure 1. The effective potential V^{eff} at high T (top left), at the nucleation temperature T_S where S obtains a non-zero vev (top right), at the nucleation temperature T_n where the SM Higgs obtains a vev and the S vev goes to zero (bottom left), and at $T = 0$ GeV (bottom right). The global minima are marked by black crosses. The contour lines are evenly spaced on a \log_2 scale and range from 10^6 GeV^4 (blue) to 10^9 GeV^4 (red). For this plot, we have chosen $\lambda_p = 1.56$, $\lambda_S = 0.5$, and $\mu_S^2 > 0$ is fixed by requiring that the tree level mass $m_S = 290 \text{ GeV}$ at $T = 0 \text{ GeV}$.

global minima. Typically there is a barrier between the $\langle S \rangle \neq 0$ and the $\langle H \rangle \neq 0$ minima, so that the phase transition between the two is first order. For the transition to take place, the formation and growth of bubbles of the new phase has to be energetically favourable [27], which happens at $T = T_n$, some time after the $\langle H \rangle \neq 0$ minima become the global ones. In other words, the Universe is in a supercooled state for some time. To calculate the nucleation temperatures T_S and T_n we used the publicly available **CosmoTransitions** package [28–31]. Note that since the effective potential is gauge dependent away from the minima, the calculated T_n may have a residual gauge dependence, see e.g. [32]. As is usual in the baryogenesis literature, we neglect this effect. For our illustrative parameter point, the effective potential at T_n is shown in the bottom left panel of fig. 1. At this point the \mathbb{Z}_2 symmetry is restored and, as long as $m_\chi < m_S$, χ stabilises.

The transition from a phase with unbroken \mathbb{Z}_2 and $U(1)_Y$ at very high T to the broken phase at intermediate T , and back to an unbroken phase at the electroweak phase transition is what we call the *vev flip-flop*. As we approach the present day, $T \sim 0 \text{ GeV}$ (bottom right panel of fig. 1), the $\langle H \rangle \neq 0$ minima deepen, and the Universe remains in the phase with broken electroweak symmetry and stable DM.

Dark Matter Freeze-Out.—One of the salient features of the Lagrangian in eq. (2) is that interactions between χ and the SM always involve the Yukawa coupling y_χ .

There is no *a priori* constraint on the magnitude of y_χ . We focus here in particular on the region of small $y_\chi \lesssim 10^{-3}$, where χ freezes out before the electroweak phase transition so that its abundance today is affected by the flip-flopping scalar vevs. The dominant processes that keep χ in thermal equilibrium at high temperatures are $\bar{\chi}\chi \leftrightarrow \tau_R^- \tau_R^+$, mediated by a t -channel S , and $\bar{\chi}\chi \leftrightarrow S^+ S^-$, mediated by a t -channel τ_R . S is kept in equilibrium with the thermal bath through the $\mathcal{O}(1)$ Higgs portal coupling λ_p . We can estimate the freeze-out temperature T_{fo} by equating the DM annihilation rate with the Hubble expansion rate. For $y_\chi \lesssim 10^{-3}$, χ never comes into thermal equilibrium with the SM through the interactions in eq. (2). We thus imagine that a thermal abundance of DM is produced during reheating after inflation or by other new interactions at scales far above the electroweak scale. χ freezes out when these interactions decouple, at a temperature $T_{\text{fo}} \gg m_\chi$. Its abundance at freeze-out is then several orders of magnitude larger than the value observed today, and is independent of m_χ and y_χ . After freeze-out, the DM number density tracks the entropy density until S develops a vev thanks to the flip-flopping vevs and χ begins to decay.

DM is also produced from S decay after S has frozen out. However, since we consider $\mathcal{O}(1)$ Higgs portal couplings, this produces a $\lesssim 1\%$ contribution to the final relic density [16], which we neglect.

Dark Matter Decay.—During the $\langle S \rangle \neq 0$ phase, χ mixes with the τ_R and can decay through three main channels: (1) $\chi \rightarrow \tau_R B^\mu$, (2) $\chi \rightarrow L_\tau H$, and (3) $\chi \rightarrow L_\tau (H^* \rightarrow t\bar{t}, t\bar{b})$. The third channel is relevant only when $m_\chi < m_H$, so that (2) is kinematically forbidden. Note that χ decay happens in the unbroken phase of electroweak symmetry, so top quarks are massless.

Since the scalar masses vary with temperature, the Universe may pass through a phase where $m_\chi > m_S$. In this case, even if $\langle S \rangle = 0$, there will be the decay (4) $\chi \rightarrow S \tau_R^-$. Recall that above the electroweak scale, when χ is decaying, S is still in the thermal bath, so processes with S in the final state are as good at depleting χ as those with SM particles in the final state.

In fig. 2 we show the evolution of the scalar vevs, the scalar masses and the effective present day DM relic density as the Universe cools, for an illustrative benchmark point with $m_\chi = 50$ GeV and $y_\chi = 2.58 \times 10^{-5}$. The parameters of the scalar potential are the same as in fig. 1. At the left edge of the plot, at $T = 1$ TeV, both scalar fields are without vevs, and the χ relic density is around nine orders of magnitude too large. When the temperature reaches $T_S \sim 570$ GeV the Universe transitions (via a first order phase transition) to a phase where $\langle S \rangle \neq 0$. At this point χ begins to decay, mostly through process (3), $\chi \rightarrow \tau_R B^\mu$. Most χ decays happen at temperatures just above the electroweak phase transition as the temperature drops more slowly at later times.

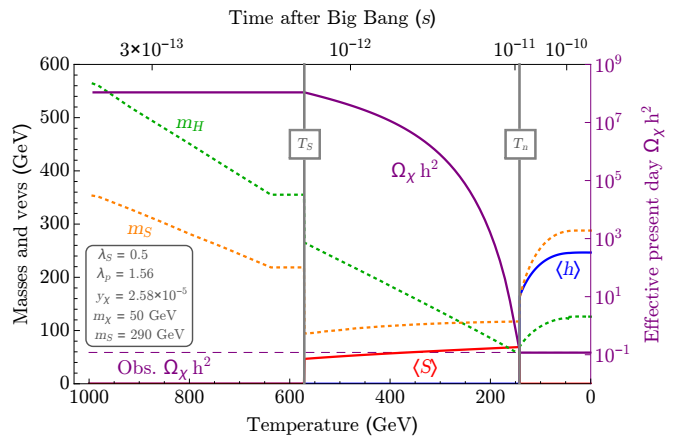


Figure 2. The vev flip-flop: at very high temperatures, both the SM Higgs field vev $\langle h \rangle$ (solid blue) and the dark sector scalar vev $\langle S \rangle$ (solid red) are zero. As the temperature drops there is a phase transition at T_S and S develops a nonzero vev, breaking the dark sector \mathbb{Z}_2 symmetry and making the DM unstable. We plot in solid purple the evolution of the effective present day relic density, obtained from the instantaneous DM number density scaled by the subsequent expansion of the Universe. At a later stage, there is a second phase transition at T_n where H develops a vev and the feedback of this vev into the dark sector via the Higgs portal restores the \mathbb{Z}_2 symmetry, halting the DM decay when the observed relic density is reached. The SM Higgs mass (dotted green) and the S mass (dotted orange) are also given.

At $T \sim 150$ GeV the $\langle S \rangle = 0$, $\langle H \rangle \neq 0$ phase becomes the global minimum, but as there is a barrier in the potential the Universe does not immediately transition to this phase; there is a short period of supercooling until the Universe nucleates to the $\langle S \rangle = 0$, $\langle H \rangle \neq 0$ phase at $T_n \sim 145$ GeV with a dramatic, first order phase transition. At this point the \mathbb{Z}_2 symmetry is restored and decays (1), (2) and (3) are no longer possible. Decay (4) is kinematically forbidden as $m_S > m_\chi$. Therefore, χ becomes stable.

Figure 2 also illustrates that the DM abundance today depends sensitively on the precise value of T_n and thus on the parameters of the model. This scenario therefore does not solve the coincidence problem between the observed baryon and DM abundances. On the other hand, if it is realised in nature, its parameters could be inferred with high precision from cosmological measurements.

In computing the χ abundance today, we take into account the momentum dependence of the decay rate. At freeze-out, χ had a Fermi-Dirac distribution, but because of relativistic time dilation, the low-momentum modes decay faster than the high-momentum ones, which leads to a skewed distribution at lower temperatures. We neglect the small decrease in the expansion rate of the Universe caused by χ decays. This is justified since χ particles are still relativistic or semi-relativistic

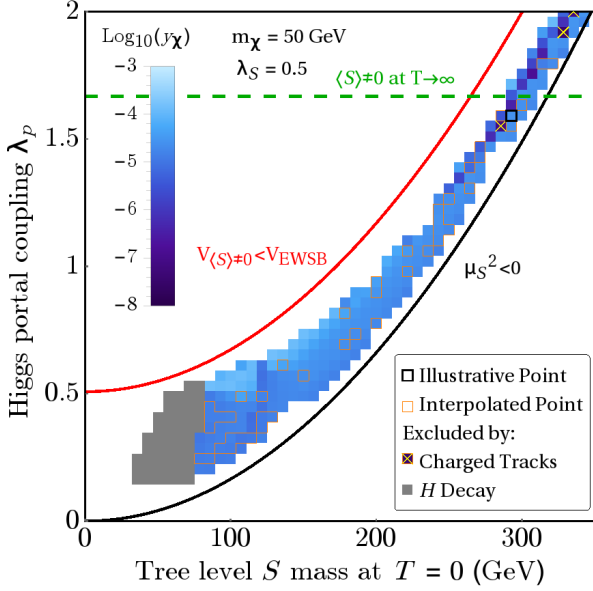


Figure 3. The y_χ values for which we obtain the correct relic density. The point bordered in black is our illustrative point used in fig. 1 and fig. 2. Orange borders are given to points which were estimated by interpolation. Points in grey have $m_S \lesssim m_H/2$ at $T = 0$ GeV, so are likely excluded by measurements of the $h \rightarrow \tau^+\tau^-$ branching ratio. The points with a yellow cross may be ruled out by searches for long lived charged particles at the LHC. Above the dashed green line the \mathbb{Z}_2 symmetry is broken in the high T limit. The red and black lines give tree level estimates for the region where the vev flip-flop is realised.

when decaying, so the entropy density injected into the thermal bath is small compared to the entropy density of the SM sector.

Parameter Space.—We now depart from the particular parameter point considered in figs. 1 and 2 and consider in fig. 3 a wider range of parameter space: the m_S – λ_p plane for $m_\chi = 50$ GeV and $\lambda_S = 0.5$. Here, m_S refers to the tree level S mass at $T = 0$. Note that for $\lambda_p \gtrsim 5$ the perturbative expansion may no longer be reliable [12, 33], but for the λ_p values shown in fig. 3 there is no problem.

We highlight the regions where the observed relic density can be obtained from the vev flip-flop, with the colour-code indicating the requisite value of y_χ . We see that for the bulk of the allowed parameter space the observed relic density is obtained for $y_\chi \sim 10^{-5}$ – 10^{-4} . In a small region at large m_S , y_χ can be as small as 10^{-10} . These points feature a long phase of supercooling before the electroweak phase transition, with a nucleation temperature $T_n \lesssim 50$ GeV. Given that $t \propto T^{-2}$ in the radiation-dominated era, the Universe spends a comparatively long time at these low temperatures. To neverthe-

less retain a DM abundance consistent with observation, the χ decay rate must be suppressed by lowering y_χ .

Below the black line in fig. 3, μ_S^2 is negative at tree level, so the \mathbb{Z}_2 symmetry is never broken at tree-level. Above the red line, $\mu_S^2 > 0$ is so large at tree level that the Universe never leaves the $\langle S \rangle \neq 0$, $\langle H \rangle = 0$ phase, implying unstable DM and no electroweak symmetry breaking. By comparing to the edge of the coloured region, we see that these tree level estimates are good approximations for the full one-loop T dependent behaviour. Above the dashed green line, our model is in the phase with broken \mathbb{Z}_2 and $U(1)_Y$ symmetries in the $T \rightarrow \infty$ limit. In this regime, the positive daisy corrections to μ_S^2 are larger than the negative one-loop corrections in the high- T limit. In principle, χ decays are then sensitive to higher scale physics, but since most decays still happen just above the electroweak phase transition, our calculations, which begin at $T = 1$ TeV, remain valid. Note that for some viable parameter choices, **CosmoTransitions** is unable to follow the evolution of the minima of our V^{eff} due to numerical pathologies. This is not a physical effect, so we estimate y_χ at these parameter points by interpolating from surrounding points. The gaps filled in this way are shown with an orange boundary in fig. 3.

Constraints and Future Tests.—The flip-flopping vevs model presented here is mainly constrained by collider searches as direct and indirect detection of χ are hindered by the smallness of y_χ , and in the case of direct detection by the leptophilic nature of χ .

At the LHC or a possible future collider, however, opportunities for discovery are manifold. First, we note that for $m_S \lesssim m_H/2 \sim 63$ GeV (indicated in grey in fig. 3), the decay mode $h \rightarrow S^+S^- \rightarrow \chi\bar{\chi}\tau^+\tau^-$ is open. Even though, to the best of our knowledge, there is no dedicated search for such decays, we surmise that it would significantly affect the measured rate for $h \rightarrow \tau^+\tau^-$ [34, 35].

Another channel that constrains the flip-flopping vevs scenario is Drell–Yan production of S^+S^- pairs through their electromagnetic interaction, followed by $S \rightarrow \chi\tau$ decay. This final state is very similar to the supersymmetric $\tilde{\tau}_R^+\tilde{\tau}_R^-$ one studied in ref. [36]. We see from fig. 9 in this reference that the data from LHC Run I is not quite sufficient yet to impose constraints. With the higher energy and higher luminosity afforded by Run II, on the other hand, the LHC should begin to cut deeply into the allowed parameter space.

For very small $y_\chi \lesssim 10^{-7}$, the decay length for $S \rightarrow \chi\tau$ becomes macroscopic and the above constraints no longer apply. Instead, searches for anomalous charged tracks are sensitive and can most likely rule out such parameter points [37–39].

Parameter points with small y_χ typically involve a large amount of supercooling. They thus admit

electroweak baryogenesis [40–43], which requires $\langle H \rangle / T|_{T=T_n} \gtrsim 1$ [12, 41, 44]. (Electroweak baryogenesis also requires a new source of CP violation, which our model in its simplest form does not offer.)

Summary.—We have presented a novel mechanism for generating the observed relic abundance of electroweak scale DM utilising a temporary period of dark matter decay at the weak scale. In this scenario, the DM abundance today is entirely governed by the dynamics of the scalar potential. We have demonstrated the mechanism in a simple Higgs portal model, focusing on a large region of parameter space where dark matter freezes out while relativistic. The initial overabundance is depleted after the \mathbb{Z}_2 symmetry that stabilises dark matter is spontaneously broken and DM decays, mainly through mixing with SM leptons. At a later point the Universe undergoes a first order phase transition that restores the dark sector \mathbb{Z}_2 symmetry and breaks electroweak symmetry. Finally, we have outlined avenues for testing this scenario at the LHC.

Acknowledgements.—We would like to thank the members of the DFG Research Unit “New Physics at the LHC”, especially Jan Heisig and Susanne Westhoff, for many useful discussions. We are moreover indebted to Jonathan Kozaczuk for invaluable advice on using *CosmoTransitions*. JK would also like to thank Moshe Moshe for interesting conversations. MB (JK) would like to thank CERN (Fermilab) for kind hospitality and support during the final stages of this project. This work was in part supported by the German Research Foundation (DFG) under Grant Nos. KO 4820/1–1 and FOR 2239, and by the European Research Council (ERC) under the European Union’s Horizon 2020 research and innovation programme (grant agreement No. 637506, “ ν Directions”).

Appendix A: The Scalar Potential at Finite T .

Here we give the finite temperature corrections to the scalar potential in eq. (1). These corrections are dominated by contributions from the scalars (h , S and the Goldstone bosons G), the W and Z bosons and the top quark. Their field dependent masses are [45, 46]

$$m_{h,S}^2(h, S) = \frac{1}{2} \left\{ (3\lambda_H + \lambda_p)h^2 + (3\lambda_S + \lambda_p)S^2 - \mu_H^2 - \mu_S^2 \mp \left[((3\lambda_H - \lambda_p)h^2 - (3\lambda_S - \lambda_p)S^2 - \mu_H^2 + \mu_S^2)^2 + 16\lambda_p^2 h^2 S^2 \right]^{\frac{1}{2}} \right\}, \quad (3)$$

$$m_G^2(h, S) = \lambda_H h^2 - \mu_H^2 + \lambda_p S^2, \quad (4)$$

$$m_W^2(h, S) = g^2 h^2 / 4, \quad (5)$$

$$m_Z^2(h, S) = (g^2 + g'^2) h^2 / 4, \quad (6)$$

$$m_t^2(h, S) = y_t^2 h^2 / 2. \quad (7)$$

Here, y_t is the top quark Yukawa coupling and g and g' are the SM $SU(2)_L$ and $U(1)_Y$ coupling constants, respectively.

The T -independent Coleman-Weinberg contribution is [21, 24]

$$V^{\text{CW}}(h, S) = \sum_i \frac{n_i}{64\pi^2} m_i^4(h, S) \left[\log \frac{m_i^2(h, S)}{\Lambda^2} - \frac{3}{2} \right], \quad (8)$$

where the sum runs over $i \in \{h, S, G, W, Z, t\}$ and $n_h = n_S = 1$, $n_G = 3$, $n_W = 6$, $n_Z = 3$ and $n_t = -12$ account for their degrees of freedom. We take the renormalisation scale Λ to be the SM Higgs vev $v = 246$ GeV.

The one-loop finite temperature correction is [22]

$$V^T(h, S) = \sum_i \frac{n_i T^4}{2\pi^2} \int_0^\infty dx x^2 \times \log \left[1 \pm \exp \left(- \sqrt{x^2 + m_i^2(h, S)/T^2} \right) \right], \quad (9)$$

where the sum runs over $i \in \{h, S, G, W, Z, t\}$. The negative sign in the integrand is for bosons while the positive sign is for fermions.

The bosons contribute to higher order *daisy* diagrams which can be resummed to give [23]

$$V^{\text{daisy}} = - \frac{T}{12\pi} \sum_i n_i \left([m_i^2(h, S) + \Pi_i(T)]^{\frac{3}{2}} - [m_i^2(h, S)]^{\frac{3}{2}} \right), \quad (10)$$

where the bosonic thermal masses (Debye masses) are given by

$$\Pi_h = (g^2/4 + 3\lambda_H/2 + y_t^2/4 + \lambda_p/6)T^2, \quad (11)$$

$$\Pi_S = (\lambda_S + 2\lambda_p/3)T^2, \quad (12)$$

$$\Pi_G = (g^2/4 + \lambda_H/2 + y_t^2/4 + \lambda_p/6)T^2, \quad (13)$$

$$\Pi_W^L = \frac{11}{6}g^2T^2, \quad \Pi_W^T = 0, \quad (14)$$

$$\Pi_Z^L = \frac{11}{6}g^2T^2, \quad \Pi_Z^T = 0, \quad (15)$$

and the sum runs over $i \in \{h, S, G, W, Z\}$. Since only the longitudinal components of the W and Z boson contribute, $n_W^L = 2$ and $n_Z^L = 1$.

Appendix B: Dark Matter Annihilation Cross Sections.

The dominant DM annihilation channels in our toy model are $\chi\bar{\chi} \rightarrow S^+S^-$ and $\chi\bar{\chi} \rightarrow \tau_R^+\tau_R^-$. The corresponding cross sections are

$$\sigma_{\chi\bar{\chi} \rightarrow S^+S^-} = \frac{y_\chi^4}{32\pi s(s-4m_\chi^2)} \left[\frac{1}{2}(s-2m_S^2) \log \left(\frac{2m_\chi^2 + 2m_S^2 - s - \sqrt{(s-4m_S^2)(s-4m_\chi^2)}}{2m_\chi^2 + 2m_S^2 - s + \sqrt{(s-4m_S^2)(s-4m_\chi^2)}} \right) - \sqrt{(s-4m_S^2)(s-4m_\chi^2)} \right], \quad (16)$$

$$\sigma_{\chi\bar{\chi} \rightarrow \tau_R^+\tau_R^-} = \frac{y_\chi^4}{64\pi s(s-4m_\chi^2)} \left[(m_S^2 - m_\chi^2) \log \left(\frac{2m_\chi^2 - 2m_S^2 - s + \sqrt{s(s-4m_\chi^2)}}{2m_\chi^2 - 2m_S^2 - s - \sqrt{s(s-4m_\chi^2)}} \right) + \frac{[\frac{1}{2}sm_S^2 + (m_S^2 - m_\chi^2)^2] \sqrt{s(s-4m_\chi^2)}/4}{sm_S^2 + (m_S^2 - m_\chi^2)^2} \right]. \quad (17)$$

In these expressions, s is the squared centre of mass energy of the annihilation process, and we have set $m_\tau = 0$.

Appendix C: Dark Matter Decay Rates.

The decay rates for the dominant DM decay channels $\chi \rightarrow \tau_R B^\mu$, $\chi \rightarrow L_\tau H$, $\chi \rightarrow L_\tau (H^* \rightarrow t\bar{t}, t\bar{b})$, and $\chi \rightarrow S\tau_R$ are

$$\Gamma_{\chi \rightarrow \tau_R B^\mu} = \frac{g'^2 \sin^2 \theta}{32\pi m_B^2 m_\chi^3} (m_\chi^2 - m_B^2)^2 (2m_B^2 + m_\chi^2), \quad (18)$$

$$\Gamma_{\chi \rightarrow L_\tau H} = \frac{y_\tau^2 \sin^2 \theta}{16\pi m_\chi^3} (m_\chi^2 - m_H^2)^2, \quad (19)$$

$$\Gamma_{\chi \rightarrow \nu_\tau t\bar{t} + \tau_L t\bar{b}} = \frac{3y_t^2 y_\tau^2 \sin^2 \theta}{256\pi^3 m_\chi^3} \left[-\frac{5}{2}m_\chi^4 + 3m_\chi^2 m_H^2 - (m_\chi^4 + 3m_H^4 - 4m_\chi^2 m_H^2) \log \left(\frac{m_H^2}{m_H^2 - m_\chi^2} \right) \right], \quad (20)$$

$$\Gamma_{\chi \rightarrow S\tau_R} = \frac{y_\chi^2}{32\pi m_\chi^3} (m_\chi^2 + m_\tau^2 - m_S^2) \sqrt{[m_\chi^2 - (m_\tau - m_S)^2][m_\chi^2 - (m_S + m_\tau)^2]}. \quad (21)$$

Here, y_t and y_τ are the Yukawa couplings of the top quark and the τ lepton, respectively, which are related to their masses by $m_x = y_x v / \sqrt{2}$. When $\langle S \rangle \neq 0$, χ will mix with τ_R . The mixing angle is $\theta \simeq y_\chi \langle S \rangle / \sqrt{2}m_\chi$, where we have used the small angle approximation. This is justified since $y_\chi \lesssim 10^{-3}$ and $\langle S \rangle \sim m_\chi$. Since the mixing angle is small, we neglect the resulting change in the χ and τ mass eigenvalues.

* micbaker@uni-mainz.de

† jkopp@uni-mainz.de

[1] **LUX** Collaboration, A. Manalaysay, *Dark-matter results from 332 new live days of LUX data*, Identification of Dark Matter 2016 [slides](#).

[2] **PandaX-II** Collaboration, A. Tan et al., *Dark Matter Results from First 98.7-day Data of PandaX-II Experiment*, [arXiv:1607.07400](#).

[3] **Fermi-LAT** Collaboration, M. Ackermann et al., *Searching for Dark Matter Annihilation from Milky Way Dwarf Spheroidal Galaxies with Six Years of Fermi Large Area Telescope Data*, *Phys. Rev. Lett.* **115** (2015),

no. 23 231301, [[arXiv:1503.02641](#)].

[4] **AMS-02** Collaboration, C. Pizzolotto, *Positron fraction, electron and positron spectra measured by AMS-02*, *EPJ Web Conf.* **121** (2016) 03006.

[5] M. S. Madhavacheril, N. Sehgal, and T. R. Slatyer, *Current Dark Matter Annihilation Constraints from CMB and Low-Redshift Data*, *Phys. Rev.* **D89** (2014) 103508, [[arXiv:1310.3815](#)].

[6] **ATLAS** Collaboration, M. Aaboud et al., *Search for new phenomena in final states with an energetic jet and large missing transverse momentum in pp collisions at $\sqrt{s} = 13$ TeV using the ATLAS detector*, [arXiv:1604.07773](#).

- [7] CMS Collaboration, *Search for dark matter in final states with an energetic jet, or a hadronically decaying W or Z boson using 12.9 fb^{-1} of data at $\sqrt{s} = 13 \text{ TeV}$* , **CMS-PAS-EXO-16-037**.
- [8] S. Profumo, M. J. Ramsey-Musolf, and G. Shaughnessy, *Singlet Higgs phenomenology and the electroweak phase transition*, **JHEP** **08** (2007) 010, [[arXiv:0705.2425](#)].
- [9] J. M. Cline, G. Laporte, H. Yamashita, and S. Kraml, *Electroweak Phase Transition and LHC Signatures in the Singlet Majoron Model*, **JHEP** **07** (2009) 040, [[arXiv:0905.2559](#)].
- [10] J. R. Espinosa, T. Konstandin, and F. Riva, *Strong Electroweak Phase Transitions in the Standard Model with a Singlet*, **Nucl. Phys.** **B854** (2012) 592–630, [[arXiv:1107.5441](#)].
- [11] J. M. Cline and K. Kainulainen, *Electroweak baryogenesis and dark matter from a singlet Higgs*, **JCAP** **1301** (2013) 012, [[arXiv:1210.4196](#)].
- [12] D. Curtin, P. Meade, and C.-T. Yu, *Testing Electroweak Baryogenesis with Future Colliders*, **JHEP** **11** (2014) 127, [[arXiv:1409.0005](#)].
- [13] B. Patt and F. Wilczek, *Higgs-field portal into hidden sectors*, [hep-ph/0605188](#).
- [14] S. Andreas, T. Hambye, and M. H. G. Tytgat, *WIMP dark matter, Higgs exchange and DAMA*, **JCAP** **0810** (2008) 034, [[arXiv:0808.0255](#)].
- [15] V. Barger, P. Langacker, M. McCaskey, M. Ramsey-Musolf, and G. Shaughnessy, *Complex Singlet Extension of the Standard Model*, **Phys. Rev.** **D79** (2009) 015018, [[arXiv:0811.0393](#)].
- [16] A. Djouadi, O. Lebedev, Y. Mambrini, and J. Quevillon, *Implications of LHC searches for Higgs-portal dark matter*, **Phys.Lett.** **B709** (2012) 65–69, [[arXiv:1112.3299](#)].
- [17] C. Englert, T. Plehn, D. Zerwas, and P. M. Zerwas, *Exploring the Higgs portal*, **Phys. Lett.** **B703** (2011) 298–305, [[arXiv:1106.3097](#)].
- [18] L. Lopez-Honorez, T. Schwetz, and J. Zupan, *Higgs portal, fermionic dark matter, and a Standard Model like Higgs at 125 GeV*, **Phys. Lett.** **B716** (2012) 179–185, [[arXiv:1203.2064](#)].
- [19] A. Greljo, J. Julio, J. F. Kamenik, C. Smith, and J. Zupan, *Constraining Higgs mediated dark matter interactions*, **JHEP** **11** (2013) 190, [[arXiv:1309.3561](#)].
- [20] A. Beniwal, F. Rajec, C. Savage, P. Scott, C. Weniger, M. White, and A. G. Williams, *Combined analysis of effective Higgs portal dark matter models*, **Phys. Rev.** **D93** (2016), no. 11 115016, [[arXiv:1512.06458](#)].
- [21] S. R. Coleman and E. J. Weinberg, *Radiative Corrections as the Origin of Spontaneous Symmetry Breaking*, **Phys. Rev.** **D7** (1973) 1888–1910.
- [22] L. Dolan and R. Jackiw, *Symmetry Behavior at Finite Temperature*, **Phys. Rev.** **D9** (1974) 3320–3341.
- [23] M. E. Carrington, *The Effective potential at finite temperature in the Standard Model*, **Phys. Rev.** **D45** (1992) 2933–2944.
- [24] M. Quiros, *Finite temperature field theory and phase transitions*, in *Proceedings, Summer School in High-energy physics and cosmology: Trieste, Italy, June 29-July 17, 1998*, pp. 187–259, 1999. [hep-ph/9901312](#).
- [25] A. Ahriche, *What is the criterion for a strong first order electroweak phase transition in singlet models?*, **Phys. Rev.** **D75** (2007) 083522, [[hep-ph/0701192](#)].
- [26] C. Delaunay, C. Grojean, and J. D. Wells, *Dynamics of Non-renormalizable Electroweak Symmetry Breaking*, **JHEP** **04** (2008) 029, [[arXiv:0711.2511](#)].
- [27] A. D. Linde, *Decay of the False Vacuum at Finite Temperature*, **Nucl. Phys.** **B216** (1983) 421. [Erratum: **Nucl. Phys.** **B223**, 544(1983)].
- [28] C. L. Wainwright, *CosmoTransitions: Computing Cosmological Phase Transition Temperatures and Bubble Profiles with Multiple Fields*, **Comput. Phys. Commun.** **183** (2012) 2006–2013, [[arXiv:1109.4189](#)].
- [29] J. Kozaczuk, S. Profumo, L. S. Haskins, and C. L. Wainwright, *Cosmological Phase Transitions and their Properties in the NMSSM*, **JHEP** **01** (2015) 144, [[arXiv:1407.4134](#)].
- [30] N. Blinov, J. Kozaczuk, D. E. Morrissey, and C. Tamarit, *Electroweak Baryogenesis from Exotic Electroweak Symmetry Breaking*, **Phys. Rev.** **D92** (2015), no. 3 035012, [[arXiv:1504.05195](#)].
- [31] J. Kozaczuk, *Bubble Expansion and the Viability of Singlet-Driven Electroweak Baryogenesis*, **JHEP** **10** (2015) 135, [[arXiv:1506.04741](#)].
- [32] H. H. Patel and M. J. Ramsey-Musolf, *Baryon Washout, Electroweak Phase Transition, and Perturbation Theory*, **JHEP** **07** (2011) 029, [[arXiv:1101.4665](#)].
- [33] C. Tamarit, *Higgs vacua with potential barriers*, **Phys. Rev.** **D90** (2014), no. 5 055024, [[arXiv:1404.7673](#)].
- [34] ATLAS Collaboration, G. Aad et al., *Evidence for the Higgs-boson Yukawa coupling to tau leptons with the ATLAS detector*, **JHEP** **04** (2015) 117, [[arXiv:1501.04943](#)].
- [35] CMS Collaboration, S. Chatrchyan et al., *Evidence for the 125 GeV Higgs boson decaying to a pair of τ leptons*, **JHEP** **05** (2014) 104, [[arXiv:1401.5041](#)].
- [36] ATLAS Collaboration, G. Aad et al., *Search for the direct production of charginos, neutralinos and staus in final states with at least two hadronically decaying taus and missing transverse momentum in pp collisions at $\sqrt{s} = 8 \text{ TeV}$ with the ATLAS detector*, **JHEP** **10** (2014) 096, [[arXiv:1407.0350](#)].
- [37] ATLAS Collaboration, G. Aad et al., *Search for long-lived, weakly interacting particles that decay to displaced hadronic jets in proton-proton collisions at $\sqrt{s} = 8 \text{ TeV}$ with the ATLAS detector*, **Phys. Rev.** **D92** (2015), no. 1 012010, [[arXiv:1504.03634](#)].
- [38] CMS Collaboration, *Search for heavy stable charged particles with 12.9 fb^{-1} of 2016 data*, **CMS-PAS-EXO-16-036**.
- [39] CMS Collaboration, *Search for displaced leptons in the e - μ channel*, **CMS-PAS-EXO-16-022**.
- [40] V. A. Kuzmin, V. A. Rubakov, and M. E. Shaposhnikov, *On the Anomalous Electroweak Baryon Number Nonconservation in the Early Universe*, **Phys. Lett.** **B155** (1985) 36.
- [41] M. E. Shaposhnikov, *Possible Appearance of the Baryon Asymmetry of the Universe in an Electroweak Theory*, **JETP Lett.** **44** (1986) 465–468. [*Pisma Zh. Eksp. Teor. Fiz.* **44**, 364(1986)].
- [42] M. E. Shaposhnikov, *Baryon Asymmetry of the Universe in Standard Electroweak Theory*, **Nucl. Phys.** **B287** (1987) 757–775.
- [43] D. E. Morrissey and M. J. Ramsey-Musolf, *Electroweak baryogenesis*, **New J. Phys.** **14** (2012) 125003, [[arXiv:1206.2942](#)].

- [44] M. Carena, M. Quiros, and C. E. M. Wagner, *Opening the window for electroweak baryogenesis*, *Phys. Lett.* **B380** (1996) 81–91, [[hep-ph/9603420](#)].
- [45] J. Choi and R. R. Volkas, *Real Higgs singlet and the electroweak phase transition in the Standard Model*, *Phys. Lett.* **B317** (1993) 385–391, [[hep-ph/9308234](#)].
- [46] J. R. Espinosa, T. Konstandin, J. M. No, and M. Quiros, *Some Cosmological Implications of Hidden Sectors*, *Phys. Rev.* **D78** (2008) 123528, [[arXiv:0809.3215](#)].